



LIGO Laboratory / LIGO Scientific Collaboration

LIGO-T060084-00-K

*Advanced LIGO UK*

April 2006

Water-cooling System for the Electrostatic Drive Amplifier

N.A. Lockerbie

Distribution of this document:  
Inform [aligo\\_sus](mailto:aligo_sus)

This is an internal working note  
of the Advanced LIGO Project, prepared by members of the UK team.

**Institute for Gravitational Research**

**University of Glasgow**

Phone +44 (0) 141 330 5884

Fax +44 (0) 141 330 6833

E-mail [k.strain@physics.gla.ac.uk](mailto:k.strain@physics.gla.ac.uk)

**Engineering Department**

**CCLRC Rutherford Appleton Laboratory**

Phone +44 (0) 1235 445 297

Fax +44 (0) 1235 445 843

E-mail [J.Greenhalgh@rl.ac.uk](mailto:J.Greenhalgh@rl.ac.uk)

**School of Physics and Astronomy**

**University of Birmingham**

Phone +44 (0) 121 414 6447

Fax +44 (0) 121 414 3722

E-mail [av@star.sr.bham.ac.uk](mailto:av@star.sr.bham.ac.uk)

**Department of Physics**

**University of Strathclyde**

Phone +44 (0) 1411 548 3360

Fax +44 (0) 141 552 2891

E-mail [N.Lockerbie@phys.strath.ac.uk](mailto:N.Lockerbie@phys.strath.ac.uk)

<http://www.ligo.caltech.edu/>

<http://www.physics.gla.ac.uk/igr/sus/>

<http://www.sr.bham.ac.uk/research/gravity/rh.d.2.html>

[http://www.eng-external.rl.ac.uk/advligo/papers\\_public/ALUK\\_Homepage.htm](http://www.eng-external.rl.ac.uk/advligo/papers_public/ALUK_Homepage.htm)

## 1 Introduction and scope

### 1.1 Purpose

This document covers the assessment of a water-cooling system for the high voltage Electrostatic Drive (ESD) amplifiers intended for the noise prototype tests of quad suspensions for Advanced LIGO.

### 1.2 Contents

- Thermal issues
- Design of the water-cooled heatsinks.
- Thermal tests of the water-cooled heatsinks
- The need for a flow-rate monitor and display
- The flow-rate monitor's circuit diagram
- Flow-rate monitor's performance
- Conclusions
- Appendix 1: The bargraph display unit
- Appendix 2: Apparatus used for the thermal tests

## 2 References

LIGO-T050110-00-K: Electrostatic Drive Amplifier for noise prototype tests (July, 2005).

LIGO-E040109-00-K: Electrostatic drive amplifier for controls prototype tests.

LIGO-E040379-01-K: Electrostatic Actuator Drive Electronics Interface Control Document.

Apex PA94/95 data sheet is available on: <http://portal.apexmicrotech.com/mainsite/pdf/pa94u.pdf>

## 3 Thermal issues

The ESD is currently designed around the PA94 (or pin-for-pin compatible PA95) high voltage power amplifier, from Apex. Microtechnology. The circuit diagram for the ESD is detailed in document LIGO-T050110-00-K, §5.4. Using the highest voltage power rails available locally for the ESD ( $\pm 307$  V), and under no-load conditions, the static power dissipated in the ESD's PA94 amplifier has been measured to be 10.1 W. For operation using the projected  $\pm 425$  V power rails—which would enable an output signal to be generated by the ESD in the range  $\pm 400$  V (the design target)—this static dissipation would rise to 14.5 W for each PA94. It is worth noting here that by using PA95 amplifiers in place of PA94s, this static dissipation would fall by an order of magnitude, albeit at the loss of high frequency ( $\geq 20$  kHz) performance. Additional AC-, or indeed short-circuit-, dissipation would be the same in both devices, however.

The Apex thermal model for the PA94 under AC conditions has predicted quite well the actual total dissipation of the ESD for the  $\pm 307$  V power rails used, and for a load capacitance of  $\sim 2300$  pF driven with a 496 Vp-p sine wave at 16.384 kHz (producing a 58.7 mA peak current). The prediction from the thermal model was 20.8 W dissipated in the PA94, compared with the actual measured value of 20.6 W. For the target maximum ESD output of 800 Vp-p at this same frequency, using the  $\pm 425$  V supply rails mentioned above, and with a 1300 pF load (which would

give a peak current of 53.5 mA), the predicted dissipation rises to 29.7 W (PA94), or 16.7 W (PA95).

It is noteworthy that with the current-limit of the PA94 (or PA95) set to the anticipated value of 70 mA<sup>1</sup>, the power dissipated in the PA94/5 under short-circuit output conditions would be 28 W in addition to the static dissipation—i.e., approximately 42.5 W for the PA94, or 29.5 W for the PA95. As this is a condition that could occur by mischance during practical operation, it was felt that active cooling of the PA94/5 amplifiers would be beneficial from the point of view of safety—even if AC operation of the ESD at frequencies as high as 16 KHz were not to be envisaged. Rupture of the PA94/5 packaging under excessive dissipation certainly should be avoided. Therefore, it was felt that a cooling system would be needed that would be capable of coping with potentially up to ~ 40 W per PA94/5, whilst maintaining the PA94/5 at a safe operating temperature.

Earlier work detailed in technical report LIGO-T050110-00-K used fan-cooled heatsinks, which were shown to function quite satisfactorily at a total dissipation of ~ 40 W per heatsink. These would almost certainly have functioned adequately well under double this dissipation, with two PA94/95 devices per heatsink, each dissipating ~ 40 W. Unfortunately, fan-cooled heatsinks are not considered to be suitable for the cooling of electronics in Advanced LIGO, because of the level of acoustic noise the fans generate, the level of electromagnetic interference they create, and the frequency spectrum over which these effects are produced.

It was therefore proposed to investigate water-cooling. Clearly, this can be a very low noise option from an acoustical point of view, particularly as the water flow-rates that are required turn out to be quite modest. Electromagnetic interference can also be reduced to negligible levels with this type of cooling, although some kind of water flow-rate sensor is needed, as described below. Several (essentially cylindrical) commercially available water-cooled heatsinks were looked at, most of these being intended for the cooling of CPUs in PCs. Unfortunately, both the shape and size of these units precluded their use for cooling as many as six ESD amplifiers housed in the intended 19" rack enclosure. Instead, a modular heatsink in the form of a water-cooled rectangular plate was designed, built, and tested, so that it could be used directly in place of the existing fan-cooled heatsinks—with some advantage in space saving, as well. Another benefit from the plate geometry is that it can act additionally as an electrostatic shield between adjacent ESD channels.

Thus, three such heatsinks would be required to be mounted in each 19" rack enclosure, in order to cater for the six proposed ESD channels, with pairs of ESD high-voltage PCBs, together with their attendant PA94/5 amplifiers, mounted one on each side of their respective heatsink plates.

## 4 Design of the water-cooled Heatsinks.

It was recognised that hard-plumbing of the water-cooling pipework internal to the enclosure, i.e., pipework that connected the triplet of heatsinks to the water supply, would make mounting or removal of the six PCBs rather awkward within each 19" rack enclosure. And so flexible nylon tubing was chosen instead to connect the heatsinks to the water supply. 6 mm o.d. (3.8 mm i.d.) nylon tubing was looked at initially, but it was found to be insufficiently flexible within the confined space of the enclosure. For this reason 4 mm o.d. (2.5 mm i.d.) nylon tubing was chosen for the 'pipework' internal to the rack enclosure. It then became possible to move the heatsinks somewhat about their normal orientations within the enclosure, without provoking water leaks, so as to provide better access to the six PCBs. It is envisaged that access to the ESD electronics within each enclosure will be only via a removable lid to the enclosure, in order to retain EM

---

<sup>1</sup> In order to provide a sufficiently high slew-rate when driving long (high capacitance) cables.

Compliance via a single conductive gasket mounted between the lid and the rest of the enclosure. With the heatsinks and PCBs normally orientated in a vertical plane, re-orientation of any heatsink by +90°, or by -90°, brings one or other of the heatsink's PCBs uppermost, so that it lies horizontal, with easy access from above through the open lid of the enclosure. Such an arrangement is shown in Figures 1 and 2, below.

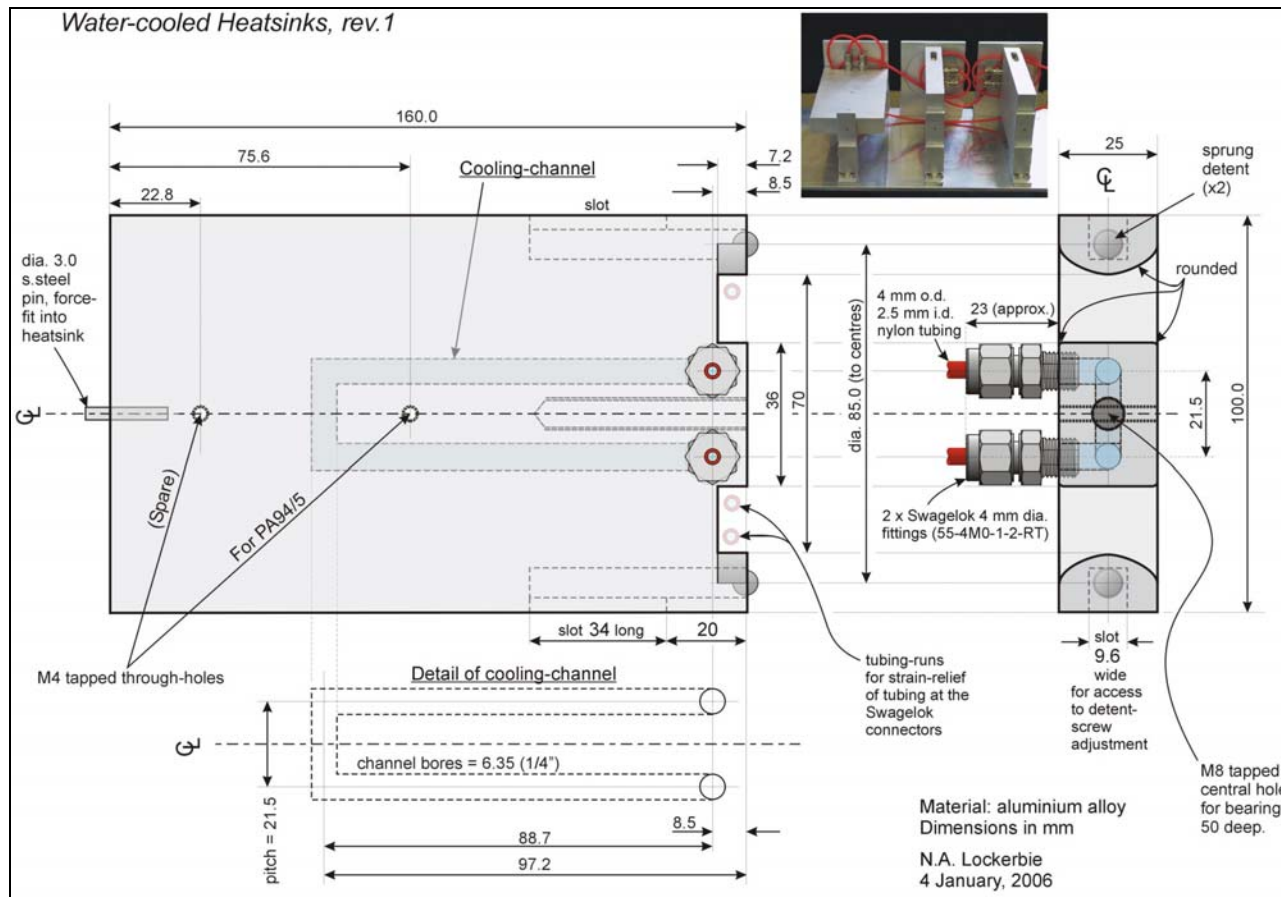


Figure 1. The modular water-cooled heatsink shown in the figure is intended to serve a pair of PCBs, each having dimensions of up to approximately 4" x 6" (100 mm x 153 mm). The PCBs will be mounted onto the two plane faces of the heatsink such that their single, centrally-positioned, high-dissipation, component (a PA94/5 power amplifier) will be cooled effectively through good thermal contact with the heatsink. The heatsink is also intended to serve as an electrostatic shield that would isolate the two PCBs from each other. The heatsink was designed to be mounted inside a standard 19" rack, the plane of the heatsink normally being vertical. For cooling purposes the heatsink carries an internal U-shaped water-channel, 1/4" in diameter, which terminates in a pair of Swagelok pipe connectors. These allow connection to 4 mm o.d. (2.5 mm i.d.) flexible nylon tubing, carrying the cooling water. Small diameter flexible tubing was used so that the heatsinks could be rotated in situ by ±90° from the vertical, if necessary (as shown in the inset photo), to provide easy access to either PCB. A pair of sprung detents lock the PCB in either the vertical or horizontal orientation.

Each 25 mm thick heatsink carries an an internal U-shaped water-channel, 1/4" in diameter, terminating in a pair of Swagelok compression pipe-connectors for attachment to the 4 mm o.d. nylon water-cooling tubing. The Swagelok connectors have tapered mounting threads, and they are screwed into the heatsinks using PTFE tape as a sealant. A central M4 tapped hole in the heatsinks allows PA94/5 amplifiers to be mounted at this location on both sides of each heatsink. A spare M4 mounting hole is also to be seen in Figure 1. The heatsinks can be rotated about a horizontal

axis, and sprung-detents lock them in either a vertical or a horizontal orientation relative to their backplates, as shown in the inset in Figure 1.

In practice it was found that with the heatsinks' water supply connecting them in parallel, partial air-locks in the tubing could—with a low driving water pressure of just 0.17 bar (using a small, local, header-tank)—cause unequal flow-rates through them. This was considered to be unacceptable, and so the heatsinks were linked together in series. No airlock problems were encountered in this configuration, and no water leaks have been detected with this plumbing arrangement either, despite using up to 1.5 bar internal water pressure, and despite considerable reorientation of all 3 heatsinks.

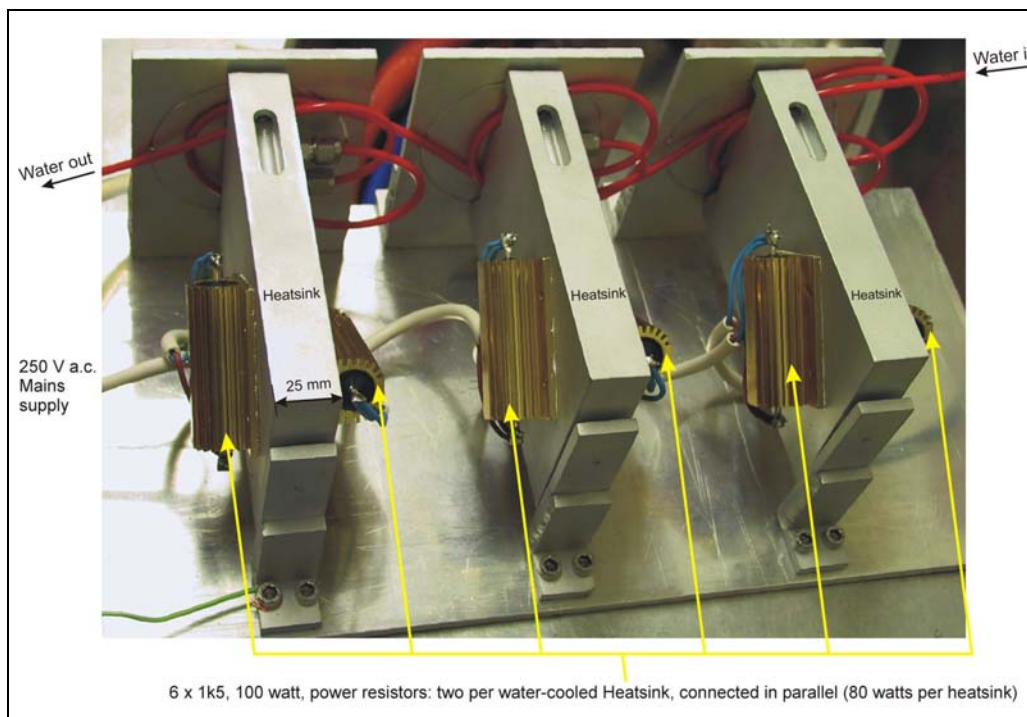


Figure 2. Six dummy loads are shown in the figure, mounted in pairs onto three water-cooled heatsinks. The six loads were labelled A–F, and the heatsinks were labelled 1–3 (both, left–right). Heatsink compound was used between each of the 1.5 k $\Omega$  load resistors and its respective heatsink. These resistors were powered from the nominally 250 V AC supply (245 V, actual), dissipating 40.0 W per load resistor. Small loops of ‘spare’ red cooling-water tubing are seen passing through apertures between each heatsink and its backplate. These fulfilled four purposes: they provided strain-relief at the Swagelok connectors, largely removing any changes in the transverse forces imparted by the tubing to these connectors (and so reducing the potential for leaks); they provided the slack needed in the tubing when re-orientating a particular heatsink; they helped to keep the water-cooling tubing tidy—close to the backplate, and out of the way; and they allowed the complete system to be purged easily of air by rotating the whole assembly so that the plane of the tubing was horizontal, and uppermost. In practice it was found that groups of three of these heatsinks should be linked together in series, as shown in the figure, rather than their being connected in parallel.

## 5 Thermal tests of the water-cooled heatsinks

Six dummy loads were attached to the three heatsinks under test, two per heatsink, each load being a 1.5 k $\Omega$ , 100 W, power resistor, as shown in Figure 2. These loads were used to simulate the actual PA94/5 amplifiers. Good thermal contact between the loads and their respective heatsinks was promoted by using a thin layer of heatsink compound under each load. The loads were

connected in parallel to the 250 V AC mains supply, via an earth-leakage circuit-breaker. In this way, 40.0 W was dissipated in each load, or 240 W, total, for the three heatsinks. The temperature of one of the ‘worst case’ load resistors, resistor ‘A’ (like ‘B’ the least well-cooled, being closest to the cooling-water outlet — please refer to Figure 2 for the nomenclature), was then monitored over time using a contactless infrared thermometer. After a period of 21 minutes the cooling-water was allowed to flow through the heatsinks, and the temperature of resistor A continued to be monitored. The resulting temperature profile over time for this resistor is shown in Figure 3. The flow-rate of

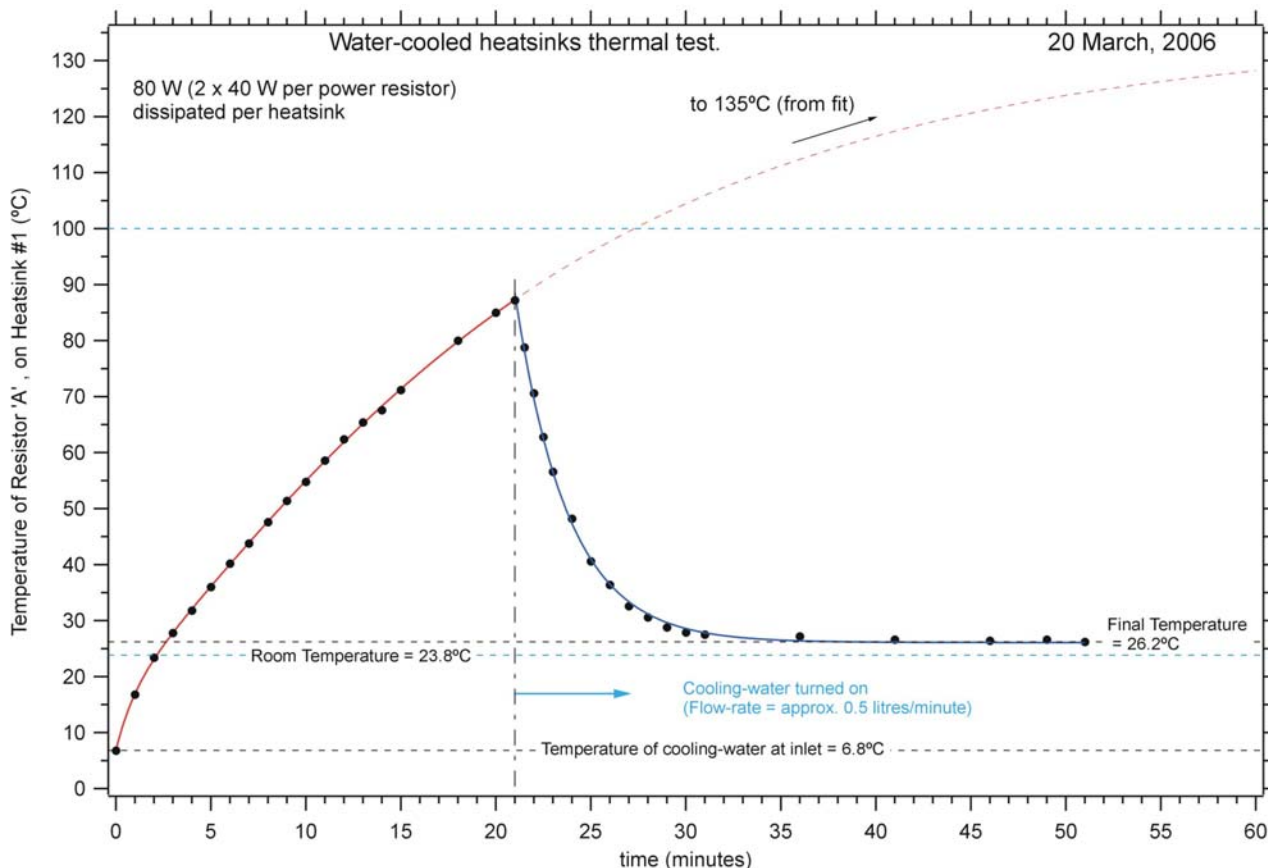


Figure 3. The thermal response of load resistor ‘A’ (the leftmost load resistor shown in Fig. 2—the one farthest from the cooling-water inlet). Mains power was applied to all six load resistors A–F at time zero, and the temperature of resistor A was monitored in the absence of, and then with, water-cooling. This cooling was turned on 21 minutes into the test. During the course of the test a total of 80 W was dissipated in the loads attached to each of the three heatsinks (40 W per load resistor, or 240 W in total). The target cooling-water flow-rate through the three series-connected heatsinks was 0.5 litres/minute. Unfortunately, it could not be kept very stable in this simple test, and it is estimated to have been maintained at the desired level  $\pm 20\%$ . Resistor A’s temperature was measured along the interior angle between the base and the body of the resistor, using a contactless infrared thermometer. Note that the temperature of the inlet cooling-water here was just 6.8 °C (Scotland !), and that in the absence of any electrical dissipation, at time zero, resistor A was cooled to a temperature close to that of the cooling-water at the inlet (within the temperature measurement error of  $\pm 0.2$  °C). The water outlet temperature was measured to be 13.7 °C at 50 minutes into the test. Resistors (A,B) ran, on average, 5.4 °C warmer than resistors (E,F) at this time, resistors (E,F) being close to the inlet of the cooling-water supply.

the cooling-water was adjusted rather crudely by cracking open or closed the cold water tap from the Physics Department building’s cold water mains supply, so as to try and maintain the flow-rate at close to 0.5 litres per minute—a very modest flow-rate. The monitoring of the water flow-rate is

described in §7, §8, and §9. The cooling water inlet and outlet temperature was also measured, periodically. Please refer to Appendix 2 for details of the apparatus used in these measurements.

From earlier tests it was found that PA94 amplifiers began to break down at a heatsink temperature of 57.5°C (LIGO-T050110-00-K), with just 20.6 W dissipated per PA94. In the case of these tests, with 40 W dissipation per load, it turned out that just prior to the cooling-water being turned on the temperature of the PA94-mimicking ‘load A’ had reached 87.2°C, although that of its heatsink (heatsink 1) was still at only 40.8°C on its upper surface at this time, due in part to the thermal lag from its relatively large thermal mass. The final limiting temperature of load A, from a double-exponential fit to the measured data, indicated a destructively high 135°C. It is therefore inferred that PA94 amplifiers mounted on these substantial heatsinks would nevertheless cease to function within some tens of minutes of operation, if subjected to these high, but conceivable, dissipations—without additional cooling, that is.

When the water-cooling was turned on, however, the temperature of load A itself (as opposed to that of its heatsink) was brought down to a cool 26.2°C. Even with cooling inlet water at a significantly higher temperature—15°C, say, rather than the 6.8°C (!) of this test—the temperature of the load (equating to that of a PA94/5’s cooling-tab) is unlikely to exceed a quite acceptable 35°C, all other conditions being equal. And it is quite possible to increase the water flow-rate above the 0.5 litres per minute that was used here (being barely a dribble, in fact), if more cooling power were needed. Indeed, a differential (inlet/outlet) water pressure of 1.5 bar doubles the flow-rate through the three heatsinks to approximately 1 litre per minute.

## 6 The need for a flow-rate monitor and display

It became obvious early on that some method of monitoring the cooling-water flow rate would be useful, in order to quantify the results obtained from the tests described above. Initially, the water run-off was just collected over a period of time, and then weighed, to find the volume flow-rate through the apparatus. This method was tedious, and a simple water flow-transducer was therefore sought, with the proviso that it have no moving magnetic parts. It was found that most, unfortunately, do use moving magnets, together with Hall-effect sensors. However, a suitable flow-transducer was found which uses an internal turbine, whose blades interrupt an infrared beam (RS Components, order code 257-149). Thus the flow-rate determines the output frequency generated by the device—in a quite linear way, in fact. This output frequency can be converted usefully into a voltage, so that the flow rate may be measured more easily over time. The circuit diagram for such an F-to-V conversion is shown in the following section. It gives a nominally 0–10 volt output for a 0–100 Hz input from the flow-transducer, using a standard tachometer IC.

The particular flow-transducer chosen has been intended for use with water, but it can also be used with light fuel oils, or weak organic acids. It has a nominal flow-rate range of 0.25–6.5 litres per minute, and although it is sized for use with standard 15 mm fittings (see Figure 5, top left), it works quite satisfactorily with a stepped adapter from 4 mm o.d. tubing. Ideally, the flow-transducer should be mounted vertically, as shown in the Figure, although even in this orientation it still will fit comfortably inside a standard 3U high rack enclosure.

Even in the best managed of water supplies there are inevitably changes in water pressure, and temperature (and so, to some small degree, viscosity, as well) over time, and it was not found to be useful to try and record the flow-rate with high accuracy. All the same, it is certainly useful to have some indication of flow-rate, and so a simple and very compact bargraph display was built around a standard IC, driving 10 low-current (500  $\mu$ A/device) LEDs, in order to give a visual indication of the water flow-rate sensed by the flow-rate monitor described in the following section. Please refer to Appendix 1, and Figure 5, for details of the bargraph display unit.





IC. This action charges/discharges the 22nF capacitor connected to pin 2 of the IC between two internally fixed voltage levels, thereby adding/removing a fixed charge to/from this capacitor. The net current flowing in this capacitor is therefore proportional to the frequency of the input signal, and this current is mirrored out of pin 3 into a 200k load resistance, so as to produce a voltage proportional to frequency. The 10µF capacitor in the Figure, together with the 200k resistance, provide the first of three stages of low-pass filtering of this voltage, i.e., of the low-frequency pulses of current coming from pin 3. These filtering stages reduce the level of ripple in the tachometer’s output. The other two stages of filtering are provided by the circuitry built around the gain-of-two op-amp, plus its emitter follower, within the IC. Note that higher-value resistors/lower-value capacitors could not be used in this 2-pole filter, because the op-amp’s input bias currents are relatively high—typically, 50 nA. DC offsets have been minimised here by presenting equal series resistance values to the two inputs of the op-amp, in the usual way.

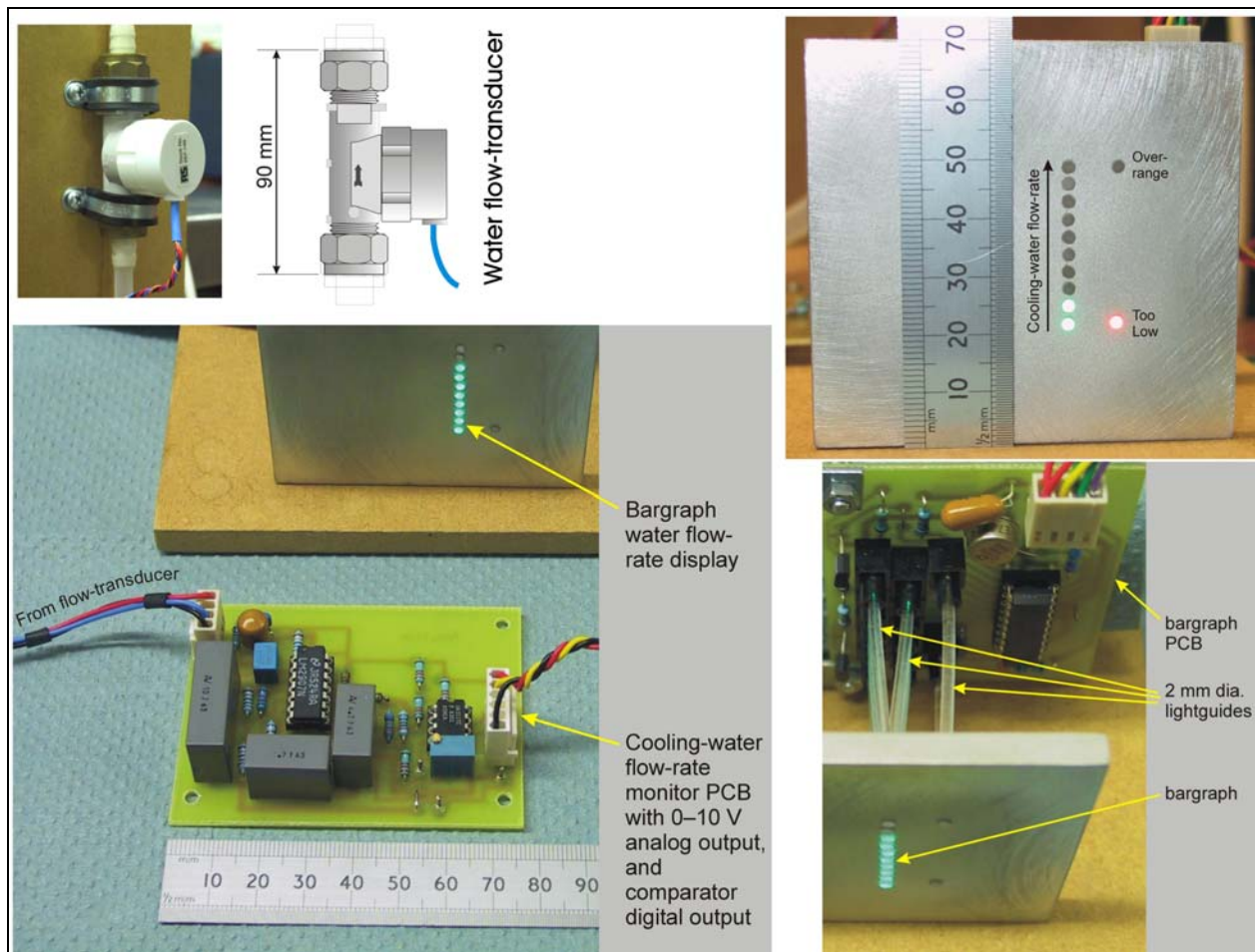


Figure 5. Top left: the water flow-transducer. Bottom left: the water flow-rate monitor circuit of Figure 4, built on a single-sided PCB measuring 77 mm × 57 mm. Top right: the compact 10-element blue-green bargraph display (< 30 mm in height), with two additional amber indicators: flow-rate ‘too-low’, and ‘over-range’. A bar having all 10 LEDs lit corresponds to a water flow-rate of at least 1.4 litres per minute. Bottom right: the 12 × 2 mm diameter light-pipes connecting the PCB-mounted LEDs to the front panel of the bargraph—giving better EMC shielding.

The final, essentially DC, output from the flow-rate monitor (0–10 V) is taken from pin 5 of the IC. This output is also applied to the input of an LM311 comparator IC, where it is compared with a preset (adjustable) lower trigger level. The comparator’s output, normally high (+12 V, approx.),

drops low (close to zero volts) if the flow-rate falls below this trigger level. The comparator's output goes high again if an adequate flow-rate is re-established, i.e., the flow-rate takes the LM2907N's output above an upper trigger level, the difference between these two trigger levels being a hysteresis of 1.1 V.

### 8 Flow-rate monitor's performance

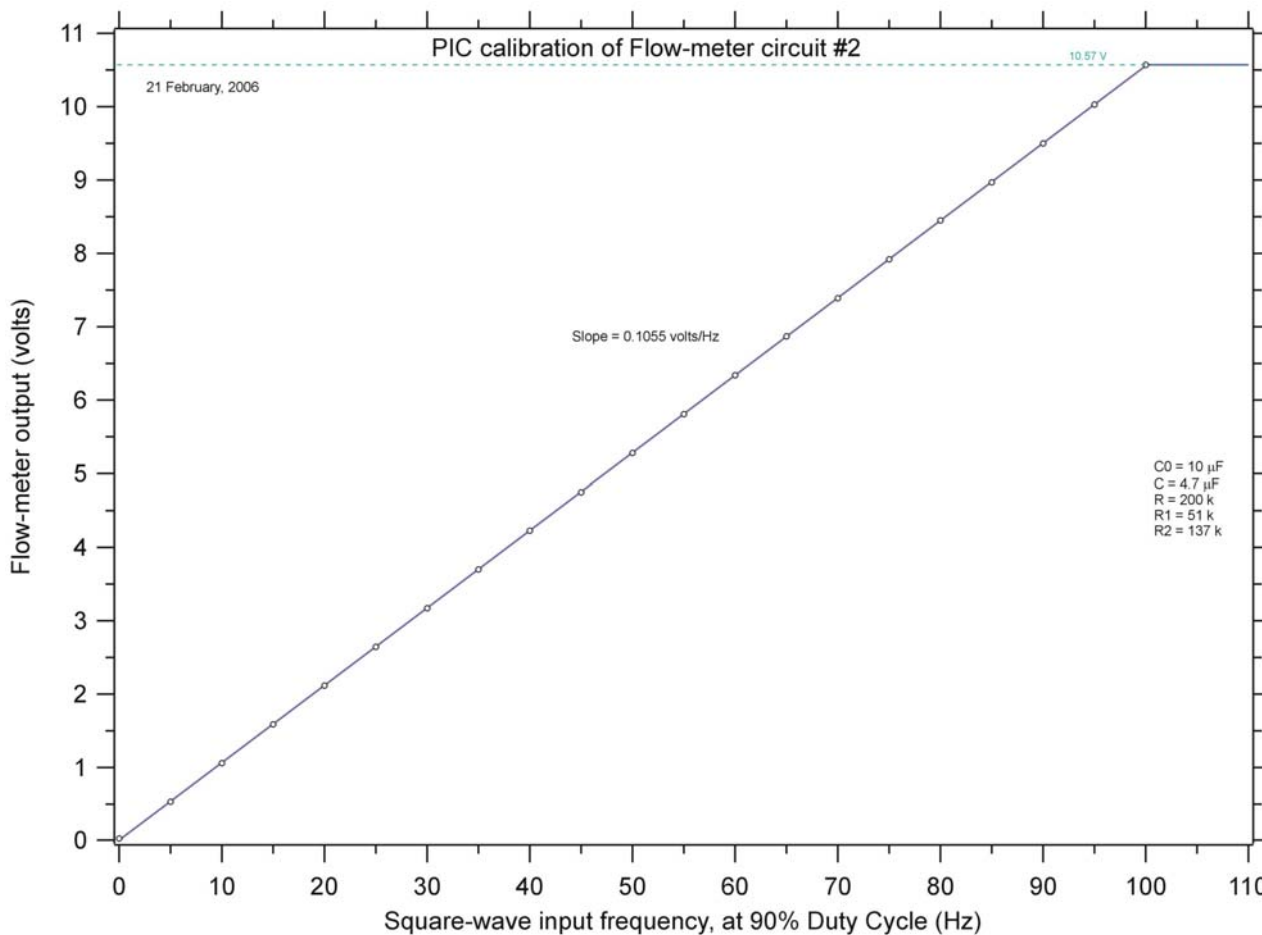


Figure 6. A PIC16F84A microcontroller was programmed (using a C cross-compiler) in order to calibrate the operation of the flow-rate monitor circuit. The calibration range of interest was from DC–100 Hz, simulating water flow-rates from zero to approximately 1.4 litres/minute, using the present flow-rate transducer. The PIC-based calibrator produced a 5 volt digital output at one of its output pins, and this was stepped up and down in frequency. The step size was 5 Hz in the range zero to 100 Hz, increasing to 100 Hz in the range 100 Hz to 500 Hz. This last range was included so as to check the proper function of the circuit for high over-range frequency inputs. The dwell-time of the PIC's output at each frequency was 15 s, and the duty-cycle at frequencies of 5 Hz and above was arranged to be 90%—in order to simulate accurately the output of the present flow-transducer. The figure shows the flow-rate monitor's voltage output to be highly linear with increasing frequency, with a negligible offset (+10 mV). Between the up- and down- sections of the frequency calibration staircase the PIC calibrator was programmed to generate a 'pulse' change in frequency from 20 Hz to 60 Hz and then back down again to 20 Hz, in order to measure the step response profile of the flow-rate monitor circuit.

The flow-rate monitor (transducer plus monitor circuit) has been calibrated, using a frequency source with a fixed 90% Duty Cycle, over the frequency range DC–500 Hz, with particular emphasis on the range DC–100 Hz. The calibrator was based upon a programmable MCU (a

PIC16F84A). The results of this calibration are shown in Figure 6—showing very good proportionality between the voltage output and the frequency input.

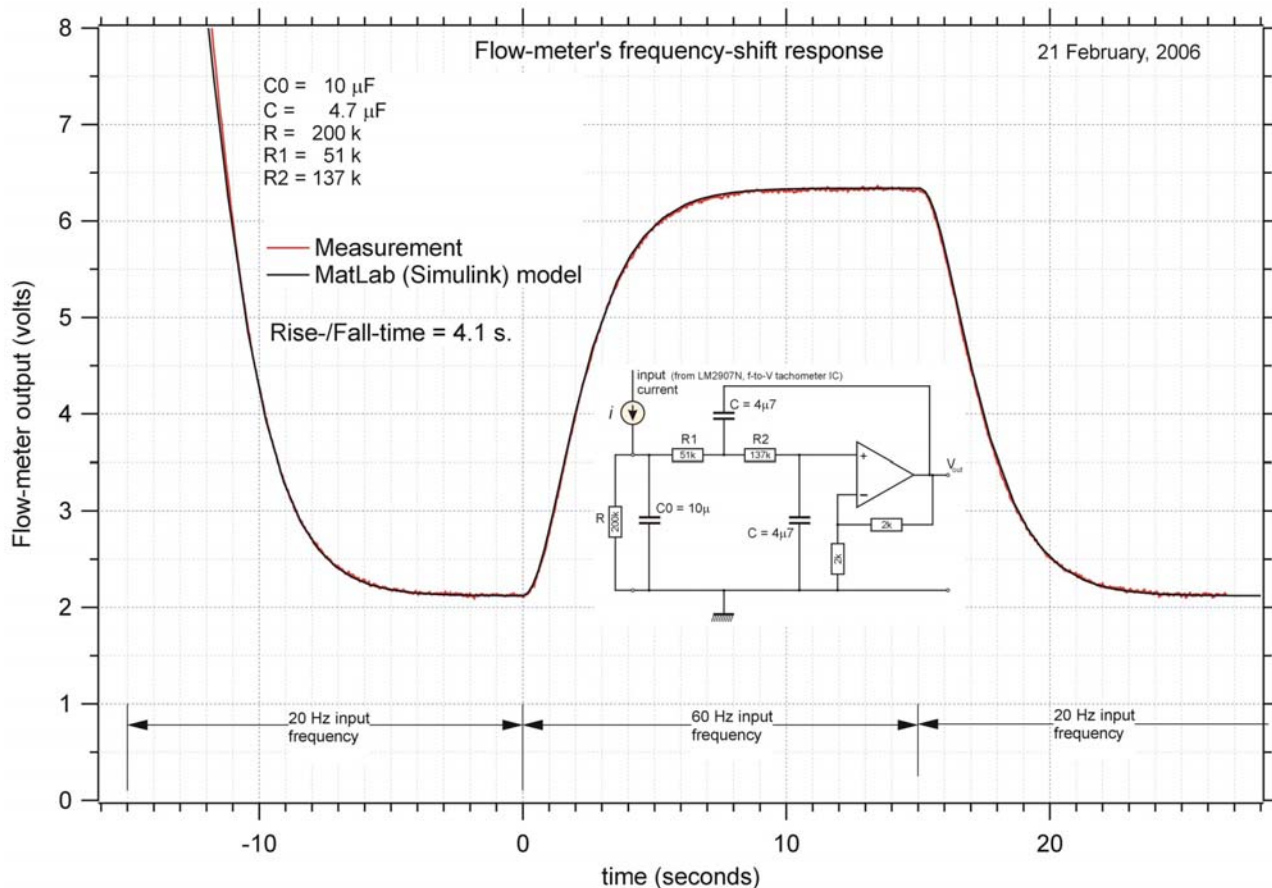


Figure 7. Mitigating the potential effect of large air bubbles in the cooling-water: the flow-rate monitor's response to a 'pulse' change in frequency. The component values of the flow-rate monitor's filter were optimised, using a Simulink model, so as to provide a relatively long rise and fall time (4.1 s) for the circuit's output response to a step-change in input frequency—which does occur when air bubbles in the cooling-water tubing pass through the flow-transducer. In this way any bubble-induced changes in the registered water flow-rate with periods  $\leq 1$  s will be reduced by a factor  $> 5$ —without any overshoot or undershoot that might very well have arisen as a result of the circuit's (effective) 3-pole response. The figure compares the measured response of the flow-rate monitor circuit with that predicted by the Simulink model.

In principle the F-to-V tachometer circuit could respond rather quickly to changes in input frequency. For example, a 60 Hz to 20 Hz drop in frequency could be detected in  $\ll 1$  s. However, it was found that if large air 'bubbles' passed through the cooling pipework of the water-cooled heatsinks with a duration  $\geq 1$  s at the flow-transducer (i.e. having a volume  $> 8$  cubic centimetres, for a flow-rate of 0.5 litres/minute) then they could cause the comparator to switch erroneously, despite its being adjusted to the lowest trigger threshold setting. For this reason the flow-rate monitor was designed to have a fairly sluggish response to step changes in input frequency. Figure 7 shows the rise and fall time of the circuit shown in Figure 4 to be  $> 4$  s. At the same time, the component values were optimised using a MatLab (Simulink) model so as to minimise any overshoot or undershoot in the circuit's step response. Figure 7 also compares the actual measured step response (in red) with that of the optimised model (black), showing generally good agreement between the two.

Finally, the flow-rate monitor was calibrated by collecting the run-off water passing through the water-cooled heatsink system over fixed intervals of time, and then weighing the accumulated

water. In this fashion the volumetric water flow rate was calculated for a number of different rates of flow. The indicated average voltage from the flow-rate monitor was also recorded during this procedure, and the resulting voltages were subsequently compared with the measured volumetric flow-rates. The results of these measurements are shown in Figure 8, below.

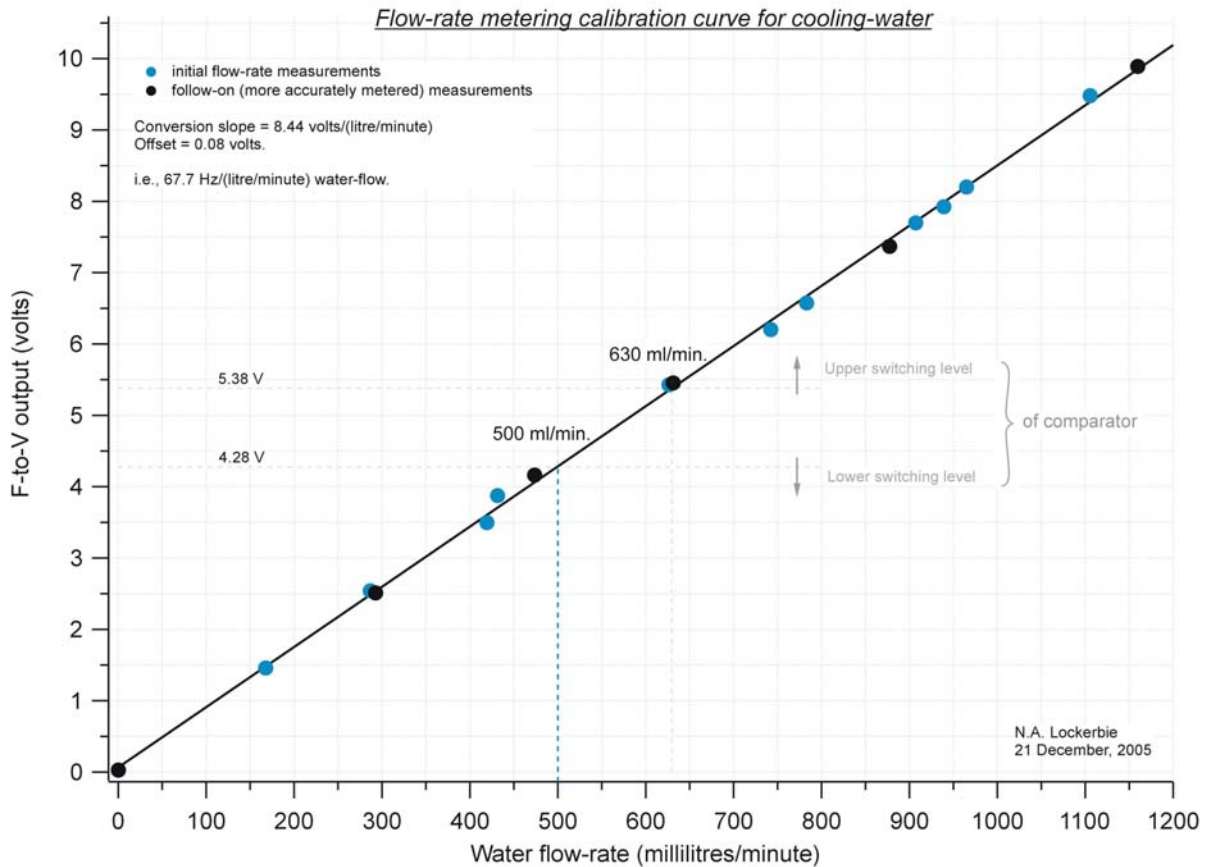


Figure 8. The water flow-rate calibration curve for the flow-rate monitor version 1 'F-to-V' (frequency to voltage) circuit. Version 2 of this circuit used high stability capacitors for the 22 n and 10  $\mu$  capacitors shown in the circuit of Fig.4., and gave an output of 7.14 volts per (litre/minute) water-flow, with a negligible offset. A full-scale 10 volt output therefore corresponded to a flow-rate of 1.4 litres/minute, for this improved version. The measured upper and lower switching levels for the comparator are shown, for an arbitrary setting of the comparator threshold, demonstrating a hysteresis of 1.1 volts (for both circuit versions 1 and 2). Note that the flow-rate transducer continued to function properly even below its rated lower range limit of 0.25 litres per minute.

Clearly, the flow-rate monitor is quite linear, this linearity even extending below the lower end of its nominal operating range at 0.25 litres per minute.

## 9 Conclusions

The water-cooled heatsink arrangement that has been tested should certainly cool the PA94/5 amplifiers adequately, even under such extreme conditions as having 40 W dissipated per device (240 W total per 19" rack-mounting enclosure). Moreover, the required cooling water flow-rate has been found to be quite modest. Indeed, a flow-rate of  $\sim 0.5$  litres per minute at a water inlet temperature of approximately 7 °Celsius has proved more than adequate, for an ambient temperature of approximately 24 °Celsius. But it is anticipated that such a flow-rate would still be sufficient even with a water inlet temperature as high as (say) 15 °Celsius. Being able to re-orientate the heatsinks seems to be a beneficial feature of using flexible tubing, and the cooling



## Appendix 2: apparatus used for the thermal tests

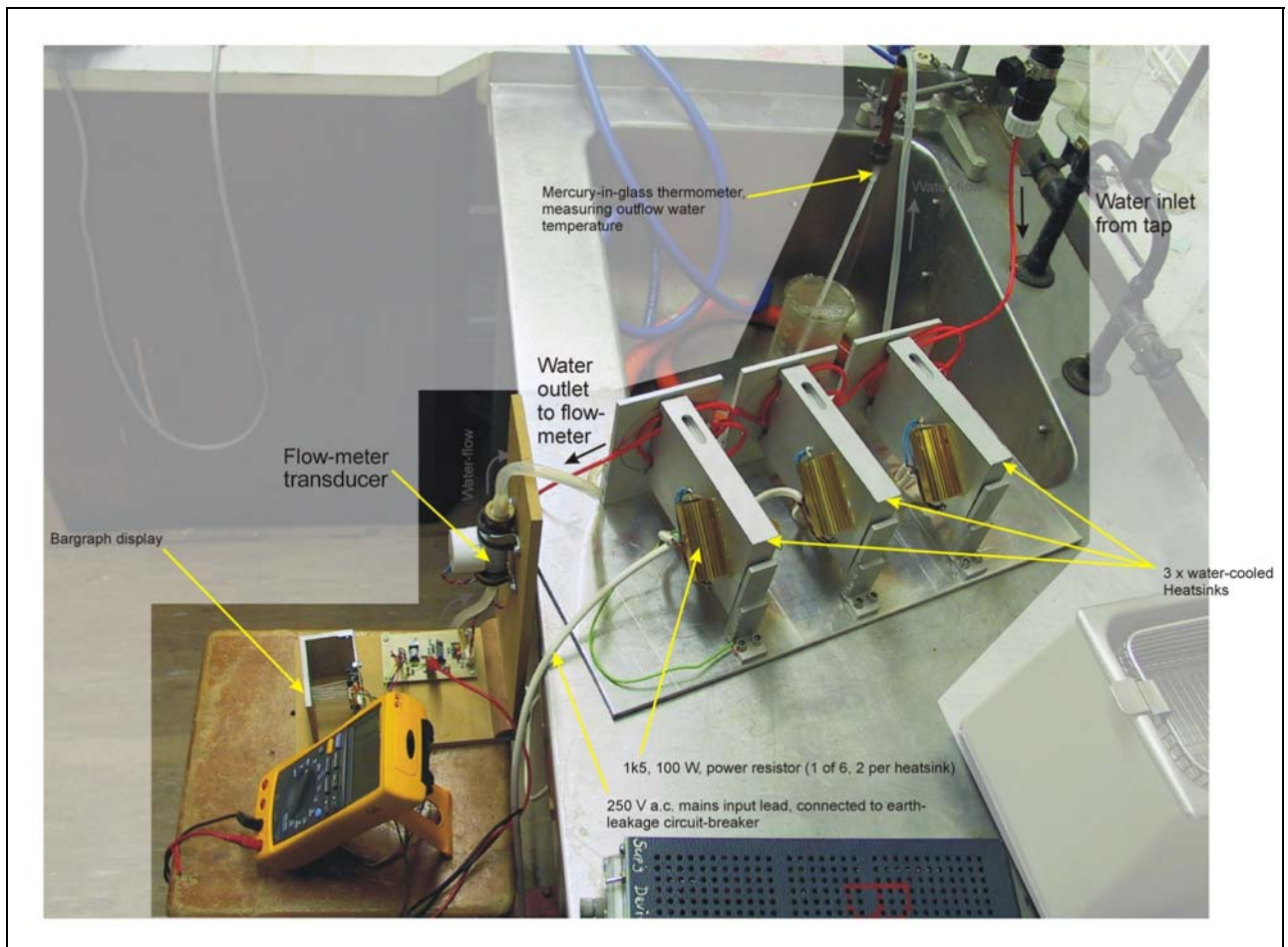


Figure 10. This shows the prototype (version 1) circuit of the flow-meter in use for the thermal tests on the water-cooled heatsinks. This version of the circuit was less compact, and used capacitors of lower stability, than the second version shown in figure 5, above. Note that the water-flow passes vertically upwards through the flow-transducer.